Free Electron Transfer from Xanthenyl- and Fluorenylsilanes (Me_3 or Ph_3) to Parent Solvent Radical Cations: Effects of Molecule Dynamics

Nikolaos Karakostas, Sergej Naumov,† Michael G. Siskos,‡ Antonios K. Zarkadis,‡ Ralf Hermann, and Ortwin Brede*

Interdisciplinary Group for Time-Resolved Spectroscopy, University of Leipzig, Permoserstrasse 15, D-04303 Leipzig, Germany

Received: September 6, 2005; In Final Form: October 18, 2005

Parent radical cations of nonpolar solvents (alkanes and alkyl chlorides) ionize 9-(trimethylsilyl)xanthenes and 9-(trimethylsilyl)fluorenes in a diffusion-controlled electron transfer. The actual electron jump as the deciding part of the process does not require a defined encounter complex, and therefore the reactants are not subjected to any geometry optimization. Considering the molecule dynamics of the donors, bending motions of the silyl group are concerted with fluctuations of the highest occupied molecular orbital electrons. Ionizing such a standing conformer mixture creates metastable (microsecond) as well as dissociative donor radical cations. A mobility restriction of the benzylic silane group in positions vertical to the phenyl plane stabilizes the radical cations and accounts for a declining amount of dissociative radical cations, which undergo C−Si bond fragmentation in the order benzylsilane > xanthenylsilane > fluorenylsilane.

1. Introduction

The high efficiency of electron transfer when radical cations of alkanes and alkyl chlorides are employed as oxidants is well-known.[1,2] Such solvent radical cations can be generated easily from radiolysis of their liquid-state solutions. As an example, the primary products of the radiolysis of *n*-butyl chloride[3] are presented in eq 1.

$$n\text{-}C_4H_9Cl \rightsquigarrow [n\text{-}C_4H_9Cl^{\bullet+} + e_{solv}^{-}] \rightarrow n\text{-}C_4H_9Cl^{\bullet+} + C_4H_9^{\bullet} + Cl^{-} \quad (1)$$

Parent radical cations ionize practically all solutes with diffusion-controlled reactions, a behavior that is being classified as free electron transfer[4] (FET) (see eq 2).

$$n\text{-}C_4H_9Cl^{\bullet+} + D \xrightarrow{FET} n\text{-}C_4H_9Cl + D^{\bullet+} \quad (D = \text{electron donor}) \quad (2)$$

Depending on the solvent and the substrate, the free energy of the reaction can vary from 0.5 to 2.0 eV.[5] Hence, FET is a very exergonic process that may take place without the formation of an encounter complex in the typical sense. In such nonpolar systems, ion solvation plays only a minor role. Then, every molecular collision leads to an electron jump regardless of the geometry of the reactants. Certainly, the limiting factor for the reaction is diffusion, which limits the experimental resolution time to the nanosecond time scale. The electron jump, however, is an early femtosecond event faster than molecular dynamics motions. Therefore, the distribution of rotational conformers of the solute is reflected directly on the secondary radical cations produced ($D^{\bullet+}$).[6,7]

SCHEME 1

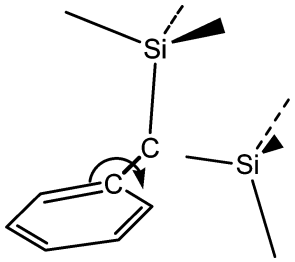

An interesting phenomenon is observed when benzyltrimethylsilane (or derivative molecules) is employed as the electron donor.

Pulse radiolysis of solutions of such silanes under conditions of FET results in the direct generation of two different transients: (i) an unstable radical cation that is desilylated instantly (in the time range of molecular vibrations) and (ii) a metastable radical cation with a lifetime of a few microseconds.[7,8] The reason for this differentiation is connected to the relative orientation of the $SiMe_3$ group with respect to the phenyl plane. The trimethylsilyl group undergoes complex vibrational and rotational movement around the benzylic bond, and conformers with all possible arrangements can be found in room temperature solutions. Experimental observations and theoretical calculations support this interpretation, but until now, there was no possibility for a clear assignment between the structure and chemical activity. In other words, we need to know in what way the conformers appearing in Scheme 1 (which are representative border cases of the molecular geometry) are responsible for the two different radical cations. A similar trend has been observed when phenol-like compounds (Ar−OH, Ar−SH, and Ar−SeH)[9] or aromatic amines[10] were subjected to FET. The mobility of the hydrogen

* To whom correspondence should be addressed. E-mail: brede@mpgag.uni-leipzig.de.
† Present address: Institute of Surface Modification, D-04303 Leipzig, Germany.
‡ Present address: Department of Chemistry, University of Ioannina, 45110 Ioannina, Greece.

10.1021/jp055028h CCC: $30.25
Published on Web 12/01/2005

TABLE 1: Substituted Xanthenes and Fluorenes Used for FET Experiments

compound	R	R_a	R_b	R_c
1x	$SiMe_3$	H	H	H
2x	$SiMe_3$	H	PhCO	H
3x	$SiMe_3$	H	PhCO	PhCO
4x	$SiMe_3$	H	MeCO	MeCO
5x	$SiMe_3$	Me	H	H
6x	$SiPh_3$	H	H	H
1f	$SiMe_3$			
2f	$SiPh_3$			

bonded to the heteroatom resulted in both instant and delayed deprotonation. However, by restriction through hydrogen bridge bonding[11] or structural fixation,[12] only the stable solute radical cation was formed.

In this paper, we report about FET ionization of fluorenyl (**f**) and xanthenyl (**x**) derivatives bearing trimethylsilyl or triphenylsilyl groups in benzylic positions. Here an unrestricted rotation of the silicon-containing group is impossible because of the molecular frame. In the case of the xanthenyl frame, the silyl group can only afford a limited bending movement, while the fluorenyl structure is rigid.

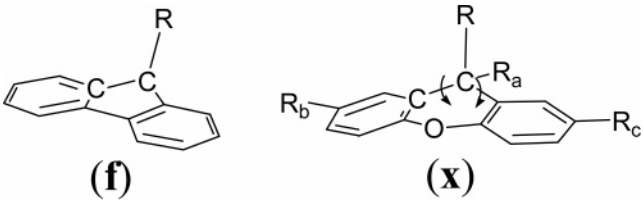

2. Experimental Section

Materials. *n*-Butyl chloride has been purified by treatment with a molecular sieve (A4, ×13) and distillation under nitrogen as described in refs 3 and 5. The fluorenyl- and xanthenylsilanes used (see Table 1) were synthesized according to the literature.[13]

Pulse Radiolysis. The liquid samples, purged with nitrogen or oxygen, were irradiated with high-energy electron pulses (1 MeV, 12-ns duration) generated by a pulse transformer electron accelerator ELIT (Institute of Nuclear Physics, Novosibrisk, Russia). Dosimetry was made using the absorption of the solvated electron in water as the calibration measurement. The dose delivered per pulse was usually around 100 Gy (which generates about 10^{-5} mol dm^{-3} of primary *n*-BuCl$^{\bullet+}$). Detection of the transient species was carried out using an optical absorption setup, consisting of a pulsed xenon lamp (XBO 450; OSRAM, München, Germany), a SpectraPro-500 monochromator (Acton Research Corp., Acton, MA), a R955 photomultiplier (Hamamatsu Photonics, Herrsching, Germany), and a 1-GHz digitizing oscilloscope (TDS 640; Tektronix, Cologne, Germany). Further details of this equipment are given elsewhere.[5] The solutions were continuously passed through the sample cell. The cell length was 1 cm.

Quantum Chemical Approach. Quantum chemical calculations were performed with density functional theory (DFT) Hybrid B3LYP[14−16] methods and a standard 6-31G(d) basis set as implemented in the *Gaussian 03* program.[17]

3. Results

Experimental Approach. Pulse radiolysis of *n*-BuCl solutions results in the formation of the solvent's radical cation; cf. reaction 1. Its optical absorption spectrum exhibits a broad band with a maximum around 500 nm and a lifetime of approximately 100 ns. When a quencher is present in millimolar concentration, this lifetime is limited to a few nanoseconds[8,18] as a result of rapid electron transfer; cf. eq 2.

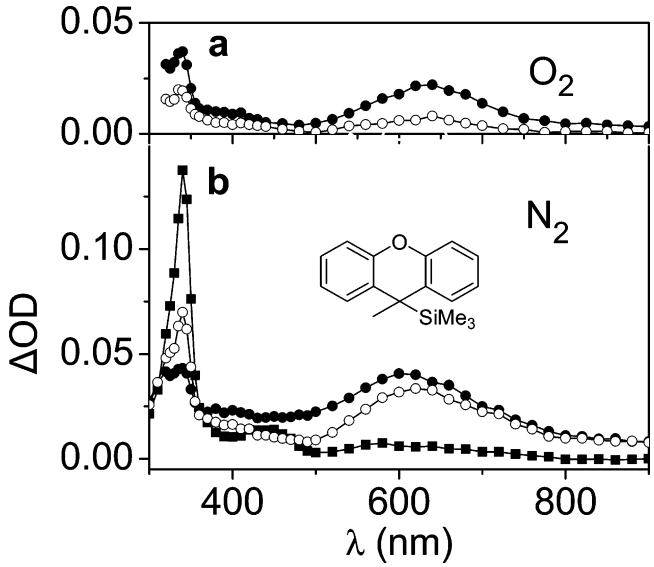

Figure 1. Absorption spectra recorded after pulse radiolysis of a 2 × 10^{-3} mol dm^{-3} solution of 9-methyl-9-(trimethylsilyl)xanthene in *n*-BuCl. Upper spectrum (a) saturated with O_2: (●) 150 ns and (○) 400 ns after the pulse. Lower spectrum (b) saturated with N_2: (●) 40 ns, (○) 90 ns, and (■) 700 ns after the pulse.

Pulse Radiolysis of Silylated Xanthenes. The transient UV−vis spectra of a pulsed 2 mmol solution of 9-methyl-9-(trimethylsilyl)xanthene (**5x**) in nitrogen-purged *n*-BuCl are presented in Figure 1b for characteristic time instances.

The spectrum recorded 40 ns after the electron pulse contains the absorption of three species. The *n*-BuCl radical cation around 500 nm is overlapped with the **5x** radical cation, which is responsible for the broad band with a maximum at 600−620 nm (extending to wavelengths higher than 900 nm) and an additional band at 320 nm. The small sharp peak at 340 nm (superimposed on the major one at 320 nm) arises from the 9-methylxanthenyl radical,[19] which has a limited contribution at this very early stage.

n-BuCl$^{\bullet+}$ is completely quenched 90 ns after the pulse, making the observation of the **5x** radical cation with a maximum at 620 nm clear. A significant buildup of the 9-methylxanthenyl radical at 340 nm can also be seen.

Finally, 700 ns after the pulse, the absorption of the 9-methylxanthenyl radical is dominant. Its formation takes place with the same time law as the decay of the **5x** radical cation (see Figure 2).

When an oxygen-saturated solution is used, the radical is drastically quenched while the bands attributed to the **5x** radical cation are marginally affected (see Figure 1a). They can, in turn, be quenched by the addition of triethylamine, a fact that serves as a confirmation of our initial assignment.

The kinetics of the electron transfer and the subsequent desilylation were analyzed at convenient wavelengths, i.e., around the transient maxima. The decay of *n*-BuCl$^{\bullet+}$ at 500 nm ($k = 1.4 \times 10^{10}$ dm^3 mol^{-1} s^{-1}) is shown in Figure 2. It is in good agreement with the formation of the **5x** radical cation observed at ∼750 nm (not shown in this paper). Because the 9-methylxanthenyl radical originates from **5x**$^{\bullet+}$, the time profile of the radical formation at 340 nm ($k_{obs} = 5.5 \times 10^6$ s^{-1}) is expected to be the mirror image of the **5x**$^{\bullet+}$ decay at 620 nm ($k_{obs} = 5.0 \times 10^6$ s^{-1}). Oxygen acts as a quencher of the transient at 340 nm with a rate constant $k = 5 \times 10^8$ dm^3 mol^{-1} s^{-1} typical for a carbon-centered radical reaction. Triethylamine

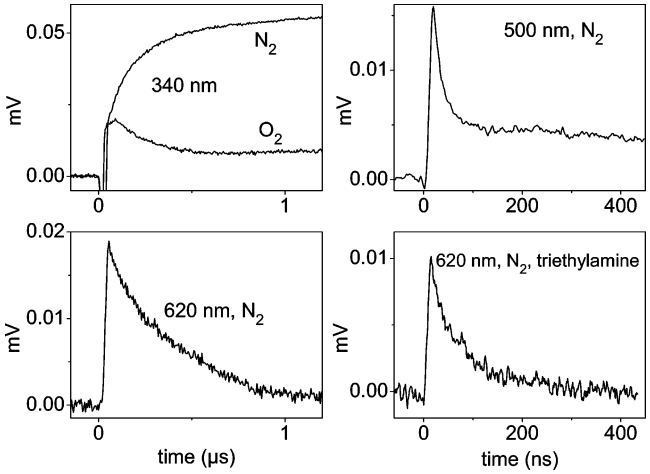

Figure 2. Time profiles derived from pulse radiolysis of 2×10^{-3} mol dm^{-3} solutions of **5x**: *n*-BuCl$^{\bullet+}$ at 500 nm; the 9-methylxanthenyl radical at 340 nm under N_2 and O_2; **5x**$^{\bullet+}$ at 620 nm in the absence and presence of 2×10^{-3} mol dm^{-3} triethylamine.

decreases the lifetime of **5x**$^{\bullet+}$ (measured at 620 nm) drastically (see Figure 2). This corresponds to a reaction rate of 4.7×10^9 dm^3 mol^{-1} s^{-1}.

In the case of benzoyl- and acetyl-substituted compounds, pulse radiolysis produces radical cations and, after cleavage of the C−Si bond, the corresponding radicals. There is a shift of their red absorption band to the IR spectral region because of extensive delocalization of the extended π system. As an example, the spectra of the transients derived from 2,7-bis(*p*-acetyl)(trimethylsilyl)xanthene (**4x**) are shown in Figure 3.

The broad band with λ_{max} at 650 nm corresponds to the radical cation **4x**$^{\bullet+}$ formed from *n*-BuCl$^{\bullet+}$. It decays with first-order kinetics ($k_{obs} = 8 \times 10^6$ s^{-1}), which can be accelerated by triethylamine addition. The sharp peak with λ_{max} at 340 nm is assigned to the 2-benzoylxanthenyl radical, though there is a degree of overlap with the tail of **4x**$^{\bullet+}$ absorption around 400 nm. The radical is formed with $k_{obs} = 1 \times 10^7$ s^{-1}, decaying slowly with second-order kinetics under N_2. Oxygen quenches the radical (see Figure 3a) but has a small influence on the **4x** radical cation because of its short lifetime ($\tau = 100$ ns). The remaining absorption around 380 nm could be caused by the resulting peroxyl radical.

Pulse Radiolysis of Silylated Fluorenes. When a 2 mmol solution of 9*H*-fluoren-9-yltrimethylsilane (**1f**) in nitrogen-purged *n*-BuCl is subjected to pulse radiolysis, FET to parent *n*-BuCl$^{\bullet+}$ results in the formation of two absorption bands with an amplitude ratio of 2:1 and λ_{max} at 355 and 635 nm (see Figure 4). They decay with first-order kinetics, exhibiting an apparent lifetimes of 1.0 μs at 635 nm and 1.2 μs at 350 nm. Because of the background absorption at 350 nm and the contribution of *n*-BuCl$^{\bullet+}$ at 635 nm, we can assume that they have the same time behavior. Oxygen has no observable effect on them. The addition of triethylamine, a typical radical-cation quencher, accelerates their decay. Because of these observations and considering previous reports for the fluorenyl radical cation,[20] they are assigned to **1f**$^{\bullet+}$. As is shown in the inset of Figure 4, when **1f**$^{\bullet+}$ is extinguished, a peak with λ_{max} at 500 nm is visible. This long-lasting species has a moderate sensitivity to oxygen ($k = 4 \times 10^7$ dm^3 mol^{-1} s^{-1}). It is attributed to the fluorenyl radical because its spectrum (see the inset of Figure 4) is identical with that reported in the literature.[21,22] Because the extinction coefficient of the fluorenyl radical (3600 mol^{-1} dm^3 cm^{-1})[22] and the concentration of *n*-BuCl$^{\bullet+}$ (1×10^{-5} mol dm^{-3}) are known, it is estimated that ~20% of **1f**$^{\bullet+}$ is decaying by C−Si bond cleavage.

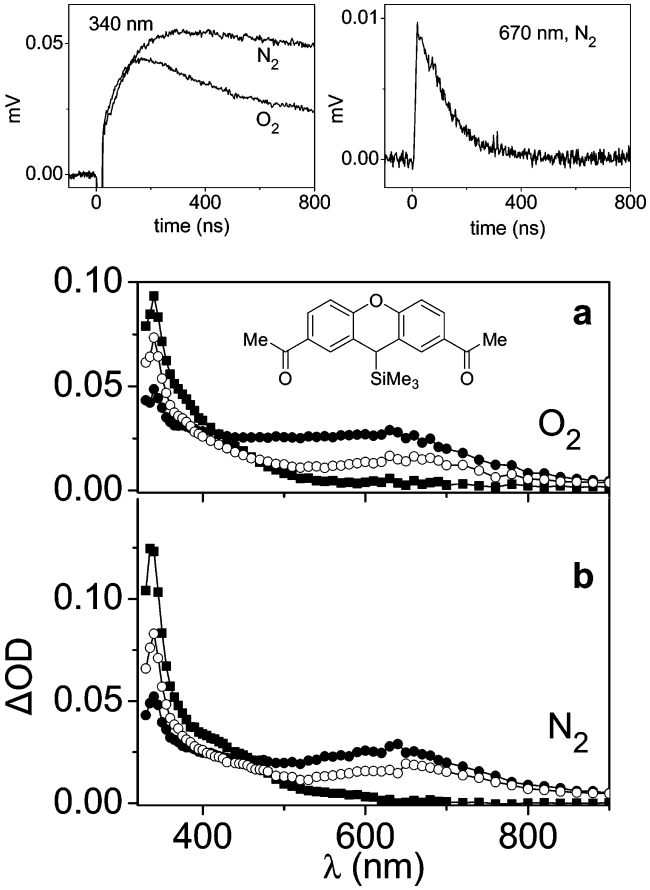

Figure 3. Absorption spectra recorded after pulse radiolysis of a 1×10^{-3} mol dm^{-3} solution of **4x** in *n*-BuCl. Upper spectrum (a) saturated with O_2: (●) 60 ns, (○) 100 ns, and (■) 200 ns after the pulse. Lower spectrum (b) saturated with N_2: (●) 60 ns, (○) 100 ns, and (■) 450 ns after the pulse. Time profiles taken at 340 nm for the 2-benzoylxanthenyl radical and at 670 nm for **4x**$^{\bullet+}$.

4. Discussion

The experimental observations regarding FET with **5x** require a reaction scheme that takes into account the fact that there are two separate paths leading to radical formation. This is supported from the spectra of Figure 1b with a rapid radical buildup (in the time range of electron transfer) and a slower one that is synchronized with the decay of **5x**$^{\bullet+}$. This is also evident from the time profiles at 340 nm, as in Figure 2, with two distinct generation methods under N_2 and quenching of the delayed formation under O_2. This complex kinetic situation is presented in Scheme 2. The key idea is the formation of two radical cations from **5x**: a dissociative one and a metastable one. Both radical cations desilylate, giving the corresponding xanthenyl radical but with extremely different rates.

In previous reports,[7,8] it was shown that the rotation of the $SiMe_3$ group in benzyltrimethylsilane has a strong influence upon the electron distribution of the highest orbitals of the molecule. This phenomenon is enhanced in the case of radical cations; therefore, the orientation of the $SiMe_3$ group with respect to the phenyl ring accounts for the generation of radical cations (after FET) with different stabilities, i.e., metastable or dissociative ones. Free rotation around the benzylic bond is not possible for xanthenyl derivatives, but a bending movement of the central molecular ring allows certain mobility for the $SiMe_3$

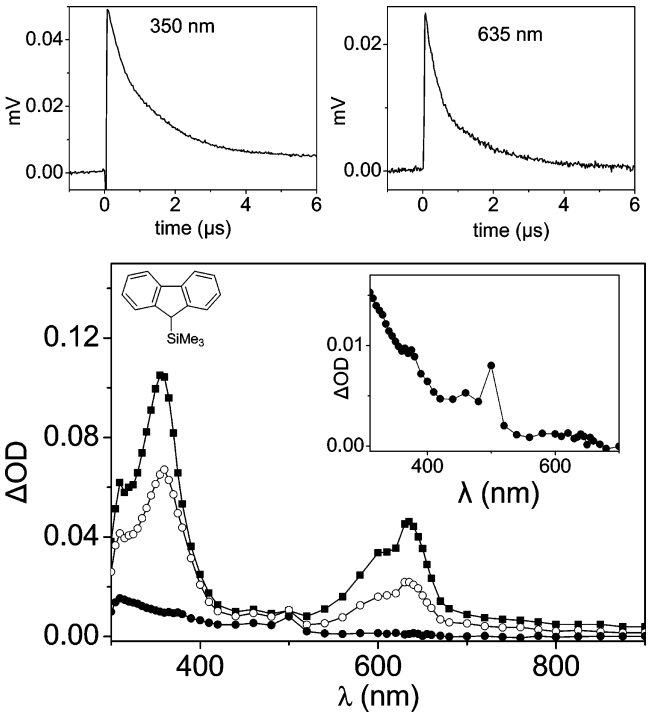

Figure 4. Absorption spectra recorded after pulse radiolysis of a 2×10^{-3} mol dm^{-3} solution of 9*H*-fluoren-9-yltrimethylsilane in *n*-BuCl saturated with N_2: (■) 150 ns, (○) 600 ns, and (●) 7 μs after the pulse. Inset: spectrum of the fluorenyl radical 7 μs after the pulse. Time profiles taken at 350 and 635 nm.

SCHEME 2

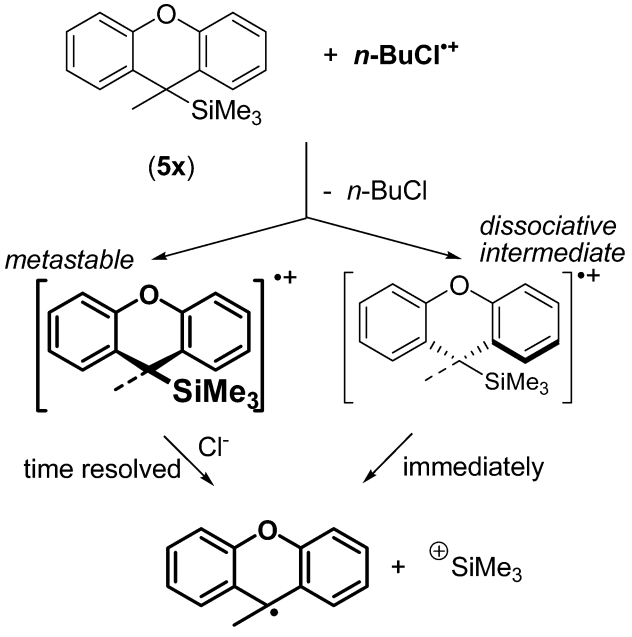

group. An analogous experimental behavior was found for compound **1x**.

In contrast to xanthenes, after FET with the fluorene **1f** only the directly observable metastable radical cations **1f** $^+$ are formed, which are subsequently (and in a delayed manner) transformed into the corresponding fluorenyl radicals, as shown in Scheme 3. This is caused presumably by the rigid molecular skeleton, which restricts the $SiMe_3$ group to an invariable position with respect to the fluorenyl plane.[23] The kinetic data for **1f** and the other compounds are summarized in Table 2.

SCHEME 3

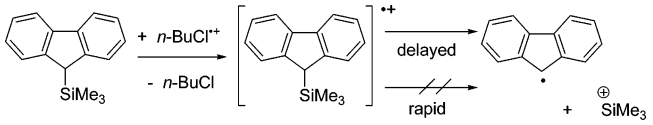

Product Distribution after FET. During the process of electron transfer to *n*-$BuCl^{\bullet+}$ from *trimethylsilylxanthene derivatives*, the formation of the corresponding radical cations as well as their desilylation products (neutral carbon-centered radicals) takes place in a concerted manner. When spectral transient superposition is absent (which is not the case here), they can be observed at separate wavelengths. If the metastable silane radical cations are eventually transformed to radicals, then calculation of the ratio between rapid and delayed radical formation is possible. This procedure becomes even more accurate when simulation of the experimental curves is used (see Figure 5) instead of a simple amplitude comparison in the time profiles of the transients. The overlapping transient absorption profiles were simulated using modified versions of the numerical integration program ACUCHEM.[24] The reaction scheme that was used included eqs 3−10. Light emission (Cerenkov light) is the reason for the small deviation between experimental and simulated curves for the first 50 ns in Figure 5a,b.

$$n\text{-BuCl} \rightsquigarrow n\text{-BuCl}^{\bullet+} + e_{solv}^- \quad (3)$$

$$n\text{-BuCl} + e_{solv}^- \rightarrow n\text{-Bu}^{\bullet} + Cl^- \quad (4)$$

$$n\text{-BuCl}^{\bullet+} \rightarrow \text{products} \quad (5)$$

$$n\text{-BuCl}^{\bullet+} + Ar_2RCSiMe_3 \rightarrow [Ar_2RCSiMe_3]_{unstable}^{\bullet+} + n\text{-BuCl} \quad (6)$$

$$n\text{-BuCl}^{\bullet+} + Ar_2RCSiMe_3 \rightarrow [Ar_2RCSiMe_3]_{metastable}^{\bullet+} + n\text{-BuCl} \quad (7)$$

$$[Ar_2RCSiMe_3]_{unstable}^{\bullet+} \rightarrow Ar_2RC^{\bullet} + SiMe_3^+ \quad (8)$$

$$[Ar_2RCSiMe_3]_{metastable}^{\bullet+} \rightarrow \text{products} \quad (9)$$

$$[Ar_2RCSiMe_3]_{metastable}^{\bullet+} + Cl^- \rightarrow Ar_2RC^{\bullet} + SiMe_3^+\text{--}Cl^- \quad (10)$$

As can be seen in Table 2, xanthene derivatives have a maximum degree of rapid desilylation of around 25% in the cases of **1x** and **5x**, which falls to 15% for the benzoylated compounds **2x** and **3x** and to 10% for the acetylated **4x**. The rapidly formed radicals appear in Figure 5a with the rate of electron transfer. The *fluorene-type molecules* **1f** and **2f** exhibit no contribution of rapid radical generation.

This unusual behavior of the substrates can be understood considering the special aspects of FET. The even distribution of charge over the σ-bond skeleton of the parent radical cation[9] (*n*-$BuCl^{\bullet+}$) in addition to the large difference in the ionization potential between the donor and acceptor ($\Delta IP > 0.5$ eV) results in a nonhindered electron jump. It occurs in every encounter of the reactants as a nonadiabatic long-range interaction without a defined encounter state in the typical sense; therefore, the molecular geometry is preserved in the products. Consequently, the distribution of radical-cation conformers does

TABLE 2: Spectral and Kinetic Parameters of Product Formation by FET from (Trimethylsilyl)xanthene and -fluorene Derivatives to *n*-BuCl$^{\bullet+}$

		silane radical cations				benzyl type radicals		
	k of FET ($dm^3\ mol^{-1}\ s^{-1}$)	λ_{max} (nm)	τ_{decay} (ns)	k_{TEA} ($dm^3\ mol^{-1}\ s^{-1}$)	k_{Cl^-} ($dm^3\ mol^{-1}\ s^{-1}$)	λ_{max} (nm)	k_{O_2} ($dm^3\ mol^{-1}\ s^{-1}$)	product ratio of radicals: rapid/delayed
1x	1.4×10^{10}	660	400	5.8×10^9	1.7×10^{10}	345	4×10^8	25/75
2x	1.5×10^{10}	680	220	6.6×10^9	7.0×10^9	345, 460	4×10^7	15/85
3x	1.5×10^{10}	660	150	6.6×10^9		360	4×10^7	15/85
4x	2.3×10^{10}	650	100	1.9×10^{10}		340	1×10^8	10/90
5x	1.4×10^{10}	620	330	4.7×10^9	2.2×10^{10}	340	5×10^8	25/75
6x	1.2×10^{10}	660	80	2×10^9		340	7×10^8	20/80
1f	2.5×10^{10}	355, 635	1000	8.4×10^9	1.5×10^{10}	500	4×10^7	−/100
2f	1.4×10^{10}	370, 600	1000	4.5×10^9	4.5×10^9	500		−/100
$PhCH_2SiMe_3$ from refs 7 and 8	5×10^9	530, 310	290			320, 260	10^9	60/40

not reflect the molecular dynamics of the transient but those of its precursor, i.e., of the parent molecule. Therefore, even some very unfavorable structures are generated. Instant fragmentation was the result of FET for 60% of the mobile benzyltrimethylsilane molecules,[7] reduced to 25% for (trimethylsilyl)xanthene, while fluorenyl-type compounds do not show any rapid radical generation. There is a clear connection between the *mobility* of the C−Si bond and the efficiency of the rapid reaction process.

Effect of Nucleophiles on Delayed Radical Formation. The observation of radical-cation decay can be associated with

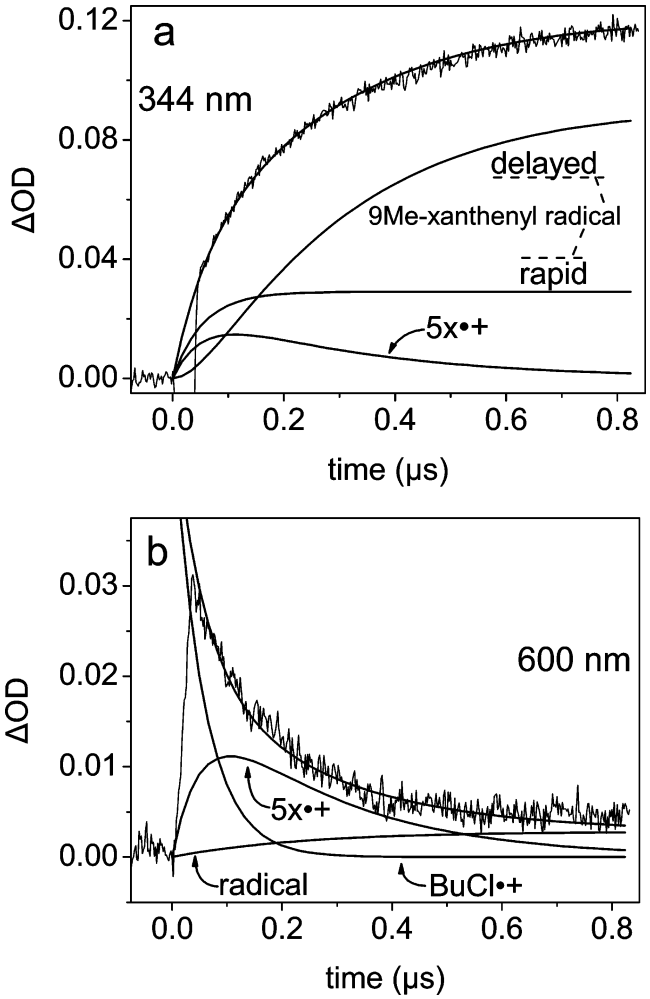

Figure 5. Time profiles depicting radical formation and simulated curves fitting the experiments: (a) at 344 nm and (b) at 600 nm for a 2×10^{-3} mol dm^{-3} solution of **5x** in *n*-BuCl under N_2.

TABLE 3: DFT B3LYP/6-31G(d) Calculated Quantum Chemical Parameters

compound	C−Si singlet (Å)	C−Si radical cation (Å)	Δ(C−Si) (Å)	spin on C−Si	IP (vertical, eV)	E_{diss}(C−Si) (radical cations)
1x	1.947	2.095	0.148	0.215	7.056	41.5
2x	1.950	2.105	0.155	0.227	7.137	40.7
3x	1.951	2.102	0.151	0.220	7.205	39.7
4x	1.950	2.101	0.151	0.222	7.423	33.8
5x	1.963	2.142	0.179	0.255	6.999	37.7
6x	1.959	2.177	0.218	0.245	6.902	18.8
1f	1.942	1.986	0.044	0.029	7.319	40.9
2f	1.940	2.004	0.064	0.027	7.162	17.3
$PhCH_2SiMe_3$	1.919[a]	2.083[a]	0.163[a]	0.311	7.953	38.4

[a] From ref 7.

electron transfer (repair reaction), the nucleophilic environment, and cleavage of the C−Si bond. The acceleration caused by nucleophiles suggests the involvement of a S_N2-type reaction (eq 11). There are numerous reports about similar behavior of silane radical cations in polar media.[25−29]

$$[Ar_2RCSiMe_3]_{metastable}^{\bullet+} + :Nu \rightarrow Ar_2RC^{\bullet} + SiMe_3^{+}\text{--}:Nu \quad (11)$$

Triethylamine was used both for the purpose of identification of radical-cation absorption bands and for the evaluation of the influence of nucleophiles on the various substrates. Its gas-phase ionization potential (7.47 eV)[30] is lower than that of xanthene (7.65 eV)[31] and fluorene (7.93 eV).[32] Electron transfer from triethylamine to their radical cations was not observed. This is in line with the quantum chemical calculations of Table 3 that predict a reduction of IP (∼0.6 eV) caused by the introduction of the Me_3Si group into the benzylic position. This phenomenon is known as the β-silicon effect.[33] Considering the data of Table 2, it is evident that substituting $SiMe_3$ with $SiPh_3$ has a stronger effect on k_{TEA} than substituting xanthenyl with fluorenyl. The $SiPh_3$ group of **6x** and **2f** is bulkier and delocalizes the charge of the radical cations. As a result, it reduces the reaction rates by 50% in comparison with **1x** and **1f**.

While the radical cation **6x**$^{\bullet+}$ has the lowest reactivity toward triethylamine ($k_{TEA} = 2 \times 10^9$ $dm^3\ mol^{-1}\ s^{-1}$), its lifetime (in pure *n*-BuCl) is the shortest measured (80 ns). Under our experimental conditions, such a lifetime can only be attributed to the nucleophilic properties of the solvent and to a monomolecular[34] C−Si fragmentation path (eq 12).

$$[Ar_2CHSiPh_3]_{metastable}^{\bullet+}, n\text{-BuCl} \rightarrow Ar_2HC^{\bullet} + SiPh_3^{+}(n\text{-BuCl}) \quad (12)$$

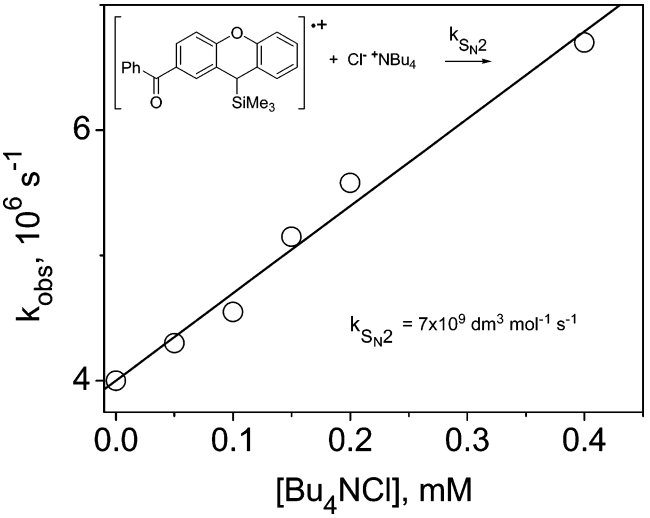

Figure 6. Plot of the pseudo-first-order rate constant for decay of $\mathbf{2x}^{\bullet+}$ formed after pulse radiolysis of a 2×10^{-3} mol dm^{-3} solution of **2x** in *n*-BuCl saturated with N_2 as a function of the concentration of tetrabutylammonium chloride.

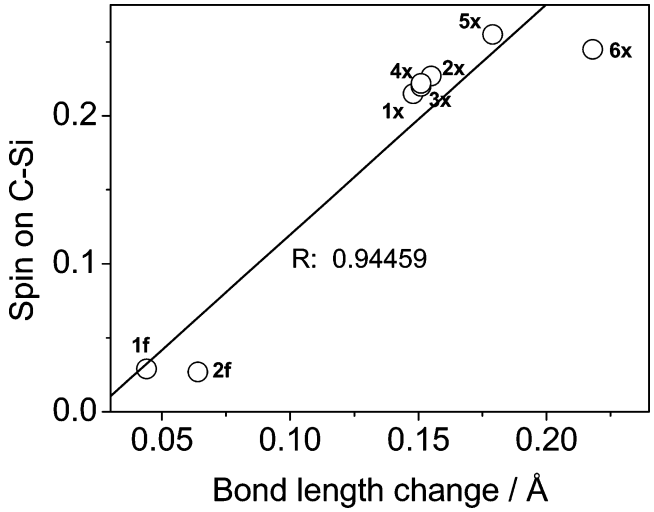

Figure 7. Plot of the calculated spin density in the C−Si bond as a function of a change in the bond length.

Absolute rate constants for the second-order reaction of silane radical cations with nucleophiles are obtained as the slopes of the plots of the pseudo-first-order rate constants for the decay of the radical cation versus the nucleophile concentration. An amount of Cl^- is formed from *n*-BuCl after irradiation (see eq 1) and can subsequently act as a nucleophile. Tetrabutylammonium chloride was used as a further source of the chloride anion. An increase in the decay rate of the radical cations was observed upon Cl^- addition, as shown in Figure 6. In the case of the fluorenylsilanes, it was accompanied by an increase in the amplitude of the fluorenyl radical produced. The xanthenyl derivatives did not exhibit any change in the radical yield. For fluorenyl radical cations, neutralization (possibly a repair mechanism) is the major decay reaction and, therefore, Cl^- enhances the generation of radicals. On the other hand, xanthenyl radical cations undergo (already) almost quantitative C−Si bond fragmentation and the addition of a nucleophile affects the process rate only.

Quantum Chemical Calculations on Energetic Relations of FET Channels. Quantum chemical calculations for all of the molecules were performed to justify the proposed reaction mechanism. It is predicted that the xanthene derivatives have a "roof-shaped" geometry with a 26° angle between the phenyl groups for the singlet ground state in the optimal conformation of compound **1x**. The trimethylsilyl group is in the axial position of the xanthenyl frame and nearly vertical to the phenyl rings (84°). The radical cations exhibit a similar geometry with a 15° angle for phenyls. The highest occupied molecular orbital (HOMO) is mainly sited on the aromatic rings, but it has a strong contribution to the C−Si bond; therefore, the bond of the radical cation is significantly prolonged (the β-silicon effect).[33]

The fluorene moiety of **1f** and **2f** in the singlet ground state adopts an almost planar configuration. The same observation holds for the radical cations. The trimethylsilyl group forms a 26° angle with the phenyls. The HOMO of fluorenylsilanes is located on the aromatic rings (see Figure 8), so the formation of the radical cations has a small effect on the C−Si bond length.

As is shown in Figure 7, there is a weak correlation between the changes of the C−Si bond length and the spin density on the two atoms. Considering the great diversity of the molecules that were studied, this is remarkable.

At room temperature for solutions of $PhCH_2SiMe_3$, the trimethylsilyl group can be found in every possible angle with respect to the phenyl group because of the low rotation E_a (3.8 kcal mol^{-1}).[7] As is shown in Scheme 4, FET results in the formation of radical cations with the same geometry as their precursors, but E_a for $SiMe_3$ rotation increases to 15.7 kcal mol^{-1}. This energy difference serves as the driving force for the C−Si bond fragmentation. The conformers that are found in the unfavorable position ($SiMe_3$ coplanar with the phenyl) dissociate in the time scale of C−Si valence vibrations (37 fs) but faster than the rotation of the $-CH_2SiMe_3$ group (0.43 ps).[7] To justify the fact that an endothermic reaction [E_{diss}(C−Si) = 38.4 kcal mol^{-1}] takes place rapidly, one should consider two important aspects: (i) the affinity of the solvent for the $^+SiMe_3$ leaving group (see eq 13b), which lowers the energy of the products[12] in comparison with gas-phase calculations, and (ii) the fact that a very exothermic process like the FET in eq 13b results in vibrationally excited states of the products[35] (thus increasing the energy level of the reactants). As a result, the energy difference can be much smaller than 22.7 kcal mol^{-1}, as depicted in Scheme 4.

$$n\text{-BuCl}^{\bullet+} + \text{PhCH}_2\text{SiMe}_3 \rightarrow [n\text{-BuCl}]^* + [\text{PhCH}_2\text{SiMe}_3]^{\bullet+}* \qquad * = \text{vibrationally excited} \quad (13a)$$

$$[\text{PhCH}_2\text{SiMe}_3]^{\bullet+}*, n\text{-BuCl} \rightarrow \text{PhCH}_2^{\bullet} + {}^+\text{SiMe}_3(n\text{-BuCl}) \quad (13b)$$

The fluorene molecular frame restricts $SiMe_3$ and $SiPh_3$ motion, eliminating any beneficial driving force for dissociation. The xanthenyl moiety exhibits a particular "butterflylike" bending motion, which makes possible a small degree of instant bond scission. The energy difference between the planar and equilibrium conformations (see Figure 8) was calculated to be 10.5 kcal mol^{-1} for **1x**. Clearly, for the rotationally restricted molecules studied in this paper, the rapid C−Si bond fragmentation is a secondary reaction. Its contribution to the reaction scheme has been reduced in xanthenes or eliminated at fluorenes in comparison with benzyltrimethylsilane.

Conclusions. FET to n-$BuCl^{\bullet+}$ is a convenient way for the generation of radical cations. In comparison with the photosensitized electron, it has two main advantages:

(i) Transient absorption spectroscopy as a monitoring technique can be used for wavelengths starting from 250 nm because the parent radical cations are metastable species with short

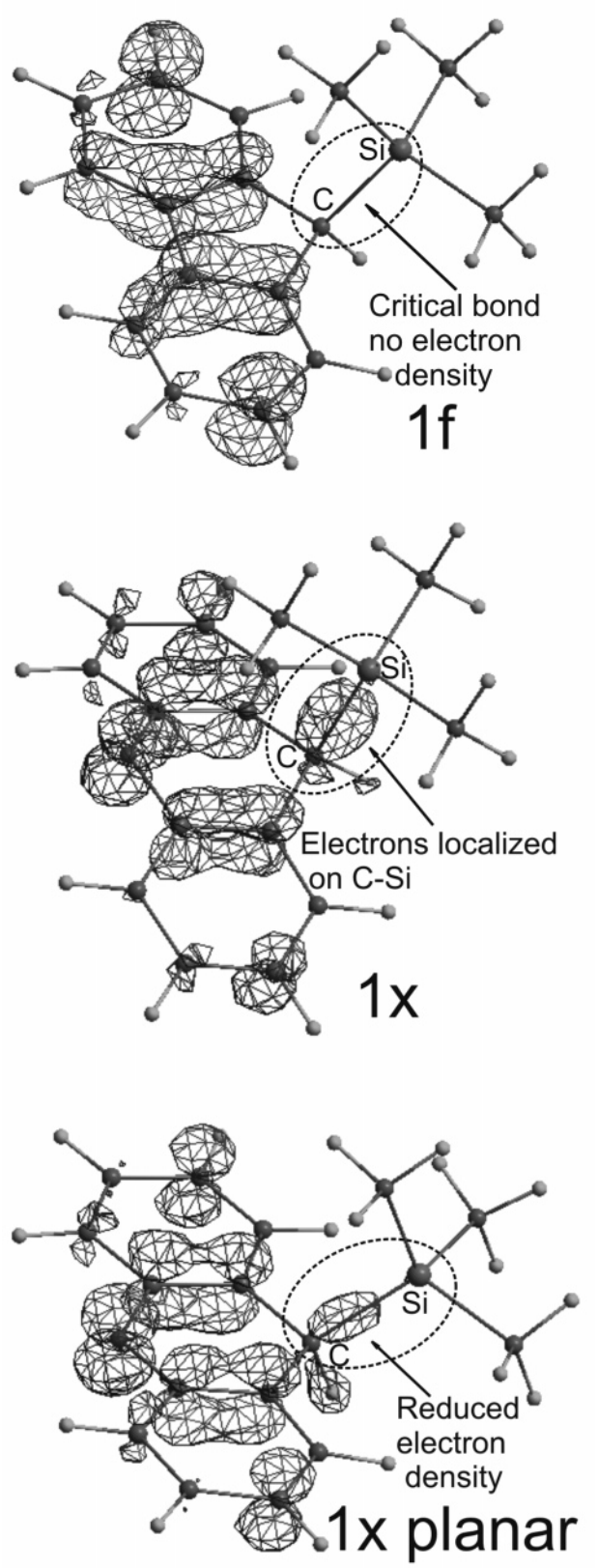

Figure 8. Electron distribution of the HOMO electrons for **1f**, **1x**, and planar **1x** configurations. The arrows point to the critical C−Si bond.

lifetimes. In photoinduced electron transfer, the sensitizer or cosensitizer (used in high concentrations) overlaps with the products and reduces the spectral range available for observations.

(ii) In photoinduced electron transfer, the formation of an encounter complex between the reactants forces the molecules into an optimal geometry that nullifies all information about their previous state. On the other hand, FET is not selective because the electron jump does not require an encounter complex. That is particularly helpful when the donor molecules bear groups (substituents) that exhibit marked electron-density fluctuations during molecular oscillations. The analysis of FET products is a way to retrieve useful information concerning electron distribution and molecular conformation.

SCHEME 4: Dissociation of Benzyltrimethylsilane after FET

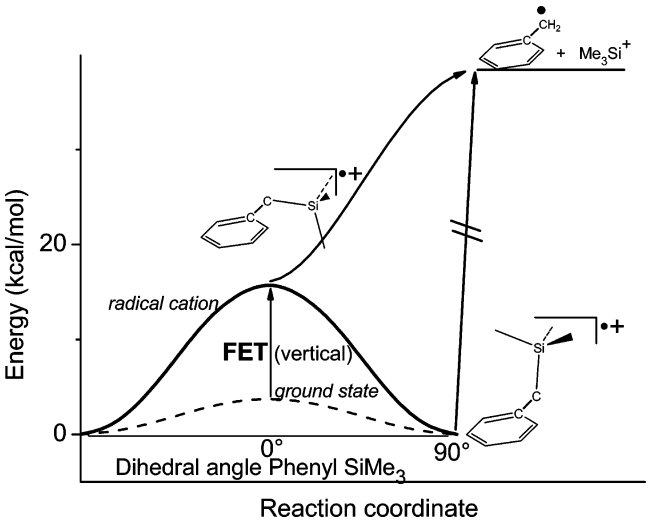

In the case of benzylsilanes, we were able to prove that restrictions on the mobility of the benzylic silane change the reactivity of the molecules. If SiR_3 is vertical to the phenyl plane, then (after FET) a delayed C−Si bond dissociation occurs. It is connected with the presence of nucleophiles such as Cl^- formed from *n*-BuCl after irradiation. When SiR_3 is parallel to the molecular plane, an additional destabilization of the radical cation causes also instant C−Si fragmentation. This can be associated with the electron density of the higher occupied orbitals on the C−Si bond. Bending or rotation motions (in the early picosecond time scale) drastically change the electron distribution of the particular bond. The electron jump during FET is a rapid event that triggers chemical phenomena in the time scale of molecular vibrations; i.e., it is a femtochemistry event.

References and Notes

(1) Brede, O.; Mehnert, R.; Naumann, W. *Chem. Phys.* **1987**, *115*, 279.

(2) Mehnert, R. Properties in Condensed Phases. In *Radical Ionic Systems*; Lund, A., Shiotani, M., Eds.; Kluwer Academic Publishers: Dordrecht, The Netherlands, 1991; p 231.

(3) Mehnert, R.; Brede, O.; Naumann, W. *Ber. Bunsen-Ges. Phys. Chem.* **1982**, *86*, 525.

(4) Brede, O.; Mahalaxmi, G. R.; Naumov, S.; Naumann, W.; Hermann, R. *J. Phys. Chem. A* **2001**, *105*, 3757.

(5) Mahalaxmi, G. R.; Hermann, R.; Naumov, S.; Brede, O. *Phys. Chem. Chem. Phys.* **2000**, *2*, 4947.

(6) Brede, O.; Naumov, S.; Hermann, R. *Radiat. Phys. Chem.* **2003**, *67*, 225.

(7) Brede, O.; Hermann, R.; Naumov, S.; Zarkadis, A. K.; Perdikomatis, G. P.; Siskos, M. G. *Phys. Chem. Chem. Phys.* **2004**, *6*, 2267.

(8) Brede, O.; Hermann, R.; Naumov, S.; Perdikomatis, G. P.; Zarkadis, A. K.; Siskos, M. G. *Chem. Phys. Lett.* **2003**, *376*, 370.

(9) Brede, O.; Hermann, R.; Naumann, W.; Naumov, S. *J. Phys. Chem. A* **2002**, *106*, 1398.

(10) Maroz, A.; Hermann, R.; Naumov, S.; Brede, O. *J. Phys. Chem. A* **2005**, *109*, 4690.

(11) Brede, O.; Hermann, R.; Karakostas, N.; Naumov, S. *Phys. Chem. Chem. Phys.* **2004**, *6*, 5184.

(12) Brede, O.; Maroz, A.; Hermann, R.; Naumov, S. *J. Phys. Chem. A* **2005**, in press.
(13) Georgakilas, V.; Perdikomatis, G. P.; Triantafyllou, A. S.; Siskos, M. G.; Zarkadis, A. K. *Tetrahedron* **2002**, *58*, 2241.
(14) Becke, A. D. *J. Chem. Phys.* **1993**, *98*, 5648.
(15) Becke, A. D. *J. Chem. Phys.* **1996**, *104*, 1040.
(16) Lee, C.; Yang, W.; Parr, R. G. *Phys. Rev. B* **1988**, *37*, 785.
(17) Frisch, M. J.; Trucks, G. W.; Schlegel, H. B.; Scuseria, G. E.; Robb, M. A.; Cheeseman, J. R.; Zakrzewski, V. G.; Montgomery, J. A., Jr.; Stratmann, R. E.; Burant, J. C.; Dapprich, S.; Millam, J. M.; Daniels, A. D.; Kudin, K. N.; Strain, M. C.; Farkas, O.; Tomasi, J.; Barone, V.; Cossi, M.; Cammi, R.; Mennucci, B.; Pomelli, C.; Adamo, C.; Clifford, S.; Ochterski, J.; Petersson, G. A.; Ayala, P. Y.; Cui, Q.; Morokuma, K.; Salvador, P.; Dannenberg, J. J.; Malick, D. K.; Rabuck, A. D.; Raghavachari, K.; Foresman, J. B.; Cioslowski, J.; Ortiz, J. V.; Baboul, A. G.; Stefanov, B. B.; Liu, G.; Liashenko, A.; Piskorz, P.; Komaromi, I.; Gomperts, R.; Martin, R. L.; Fox, D. J.; Keith, T.; Al-Laham, M. A.; Peng, C. Y.; Nanayakkara, A.; Challacombe, M.; Gill, P. M. W.; Johnson, B.; Chen, W.; Wong, M. W.; Andres, J.; Gonzalez, C.; Head-Gordon, M.; Replogle, E. S.; Pople, J. A. *Gaussian 03*, revision B.02; Carnegie Mellon University: Pittsburgh, PA, 2003.
(18) Brede, O. *Res. Chem. Intermed.* **2001**, *27*, 709.
(19) Siskos, M. G., private communication.
(20) McClelland, R. A.; Mathivanan, N.; Steenken, S. *J. Am. Chem. Soc.* **1990**, *112*, 4857.
(21) Wong, P. C.; Griller, D.; Scaiano, J. C. *J. Am. Chem. Soc.* **1981**, *103*, 5934.
(22) Gaillard, E.; Fox, M. A.; Wan, P. *J. Am. Chem. Soc.* **1989**, *111*, 2180.
(23) Overby, J. S.; Woofter, R. T.; Rheingold, A. L.; Incarvito, C. D.; Sommer, R. D. *J. Chem. Crystallogr.* **2003**, *33*, 357.
(24) Braun, W.; Herron, J. T.; Kahaner, D. K. *Int. J. Chem. Kinet.* **1988**, *20*, 51.
(25) de Lijser, H. J. P.; Snelgrove, D. W.; Dinnocenzo, J. P. *J. Am. Chem. Soc.* **2001**, *123*, 9698.
(26) Dockery, K. P.; Dinnocenzo, J. P.; Farid, S.; Goodman, J. L.; Gould, I. R.; Todd, W. P. *J. Am. Chem. Soc.* **1997**, *119*, 1876.
(27) Kako, M.; Nakadaira, Y. *Coord. Chem. Rev.* **1998**, *176*, 87.
(28) Ohga, K.; Yoon, U. C.; Mariano, P. S. *J. Org. Chem.* **1984**, *49*, 213.
(29) Zhang, X.; Yeh, S.-R.; Hong, S.; Freccero, M.; Albini, A.; Falvey, D. E.; Mariano, P. S. *J. Am. Chem. Soc.* **1994**, *116*, 4211.
(30) Mathis, J. E.; Compton, R. N. *J. Chem. Phys.* **1996**, *104*, 8341.
(31) Bouchoux, G.; Dagaut, J. *Org. Mass Spectrom.* **1981**, *16*, 246.
(32) Dewar, M. J. S.; Haselbach, E.; Worley, S. D. *Proc. R. Soc. London, Ser. A* **1970**, *A315*, 431.
(33) Lambert, J. B.; Zhao, Y.; Emblidge, R. W.; Salvador, L. A.; Liu, X.; So, J.-H.; Chelius, E. C. *Acc. Chem. Res.* **1999**, *32*, 183.
(34) Mella, M.; d'Alessandro, N.; Freccero, M.; Albini, A. *J. Chem. Soc., Perkin Trans. 2* **1993**, 515.
(35) Medvedev, E. S.; Osherov, V. I. *Radiationless Transitions in Polyatomic Molecules*; Springer Series in Chemical Physics 57; Springer: Berlin, 1995; p 36.